Full Length Research Paper

Linear buckling optimization and post-buckling behavior of optimized cold formed steel members

F. Kolcu[*], T. Ekmekyapar and M. Özakça

Department of Civil Engineering, University of Gaziantep, Gaziantep, Turkey.

Today's high-strength materials allow for significant increases in working and limit stresses. To fully exploit material improvements as weight savings on structures, it is desirable to enhance the performance of structural components. The work presented in this paper proposes that the buckling behavior of cold form steel columns may be effectively improved without increased material volume. In order to achieve this goal, optimization algorithm which integrates finite strip analysis, geometric modeling, semi analytical sensitivity analysis and sequential quadratic mathematical programming methods can be used to find an optimum cross section of cold-formed steel columns under axial compression. The objective is the maximization of the critical buckling load with constraints on the volume of material used. Several examples are included to illustrate advantage of the optimization. The post buckling performance of optimized cold form steel columns was also investigated using nonlinear variable thickness finite strip analysis. Non-linear finite strip analysis helped to understand the behaviour of these cold form steel columns and select the most promising designs. The optimum forms found in this paper can be used to develop improved designs for cold formed steel columns.

Key words: Cold formed steel, column buckling, optimization.

INTRODUCTION

Cold-formed steel members have been widely used in civil engineering structures. In particular, light gauge cold-formed channels are commonly used as wall studs and chord members of roof trusses in steel frame housing and industrial buildings. Their manufacturing process involves forming steel sections in a cold state (that is, without application of heat) from steel sheets of uniform thickness. Cold-formed steel structural members may lead to a more economic design than hot-rolled members as a result of their high strength to weight ratio, ease of construction and suitability for a wide range of applications.

With the increasing use of high strength steels, it is inevitable to reduce the thickness of the section. Based on the strength design criterion, the cold-formed steel member can have a very thin thickness. Thereupon, cold-formed steel sections have distinct structural stability problems, which are not observed in hot-rolled steel sections. In steel compression members, three structural

instability modes, namely local, distortional, and flexural/flexural–torsional buckling, are likely to occur. Efforts have been made to increase the buckling resistance by designing optimum sections

Under axial compression, cold formed channel columns may buckle in one of several modes including local buckling, distortional buckling, and flexural–torsional buckling (Hancock, 1985). Many theoretical and experimental studies have been conducted for determining the buckling behavior of cold formed columns (Kwon and Hancock, 1992; Kesti and Davies, 1999).

Moreover, a closed-form solution was devised by modeling a flexural–torsional buckling mode of the lipped flange elastically restrained by the web (Lau and Hancock, 1987). This closed-form solution was then verified by a Finite Strip (FS) buckling analysis and simplified for practical application. Other analytical method has been presented, namely the Euro Code 3 method, which is based on flexural buckling of the stiffener. The generalized beam theory provides a particularly good tool with which to analyze distortional buckling in isolation and in combination with other modes and has been presented in more detail (Davies and Leach, 1994). The FS method

---

*Corresponding author. E-mail: kolcu@gantep.edu.tr.

has also proved to be a useful approach, because, like generalized beam theory, it also has a short solution time compared to the finite element method and has been used for buckling analysis of cold formed sections (Schafer and Peköz, 1998). The FS method simply assumes a supported end boundary conditions and is applicable for longer sections where multiple half-waves occur in the section length. Considering appropriate modifications to the element thickness and choice of buckling half-wavelength distortional and local buckling of a cold-formed steel member with holes, are determined with the semi-analytical FS method (Cristopher and Schafer, 2009).

Experimental studies on cold-formed stainless steel columns were conducted by many researchers (Talja A and Salmi, 1995; Young and Hartono, 2002; Gardner and Nethercot, 2004). The recent major experimental research work of cold-formed stainless steel structures is summarized (Gardner and Nethercot, 2004). Base on experiments and theoretical models American (ASCE-8-02), Australian/New Zealand (AS/NZS 4673) and European (Eurocode 3) specifications enclosed the design of cold formed steel sections.

One of the prominent advantages of cold-formed steel is its flexibility in forming various cross-section shapes. However, in practice, only limited cross-sections are adopted. Among them, the C-, R- and Z-shapes are the most widely preferred by designers. Nevertheless these cross-section shapes have never been proven superior to alternatives. Actually, using the same amount of steel, it is possible to find cross-section designs with higher load capacity than the traditional C-, Z- and R-shapes by means of powerful optimization tools. Optimizing the cross-section shape of a cold-formed steel member is a comprehensive issue from a structural mechanics view-point. There has been various works in cold-formed steel member optimization presented in the literature. Gradient-based search techniques were used for the optimization of hat-shaped sections (Seaburg and Salmon, 1971). Comprehensive parametric study was performed for the global optimum of hat-shaped beams (Karim and Adeli 1999). Genetic algorithm optimization was carried out for Z- and R-shape purlins by means of FS analysis within the objective function evaluation (Lu, 2002). Also a micro genetic algorithm was adopted to find out optimum cross section for cold formed steel channel and lipped channel columns under axial compression (Lee et al., 2006). They generated some design curves for optimum values of design variables.

Compression members such as the cold form steel channel will locally buckle in a number of half-wave lengths and will retain this mode shape into the post-local buckling range, until localization occurs in one of the half-waves propagating failure. It is expected that loads at failure may be considerably higher than those at which local buckling occurs, due to the redistribution of longitu-

dinal stresses from the flexible to the stiff parts of the cold form steel section. In the past, researchers have investigated the post-buckling modes of commonly used cold-formed steel sections. A non-linear elastic analysis was studied by Kwon and Hancock (1991), Pignataro et al. (2000) and Pu et al. (1999) based on the spline finite strip / finite element methods that can handle local, distortional, and overall buckling modes in the post-buckling range and the interactions between them. It is a consequence of the increasing complexity of section shapes that buckling calculations are becoming more complicated and that post-buckling takes on increasing importance.

To fully develop and validate optimized cold form steel member section, research herein has focused on two key areas:

1. To develop and demonstrate the use of the robust and inexpensive computational procedure for finding the shape and thickness of the optimal cross-sections of cold formed steel members under buckling load. The optimization procedure is based on maximization of the critical buckling load with a constraint that the volume of the cold formed steel member material remains constant.
2. To investigate the post buckling behavior of optimized section.

The specific objective of this paper may be summarized as:

1. To observe the change in element shapes during optimization procedure to remark the efficiency of each dimension on the critical buckling load.
2. Obtain the best shape and thickness variation of cold formed steel members, so that it can carry loads without buckling.

OPTIMIZATION PROCEDURE

Cold formed steel member posses higher buckling loads for a given volume of material when properly shaped. This may be achieved by the use of structural shape optimization procedures in which the shape and thickness of the structure are varied to achieve a specific objective satisfying certain constraints. Such procedures are iterative and involve several re-analyses before an optimum solution can be achieved. Structural shape optimization tools can be developed by the efficient integration of structural shape definition procedures, automatic mesh generation, FS analysis, sensitivity analysis and mathematical programming methods. Figure 1 illustrates an overview of a typical structural optimization procedure. The main parts of the optimization algorithm are summarized below. Problems of structural optimization are characterized by various objectives
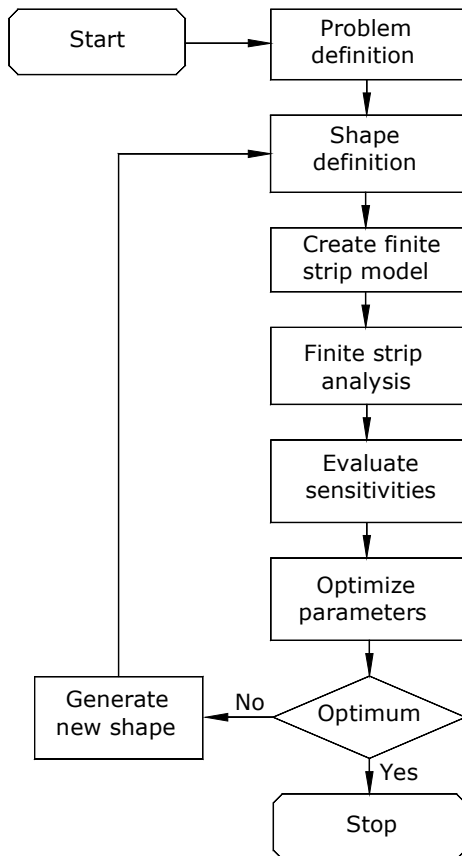
Figure 1. Structural optimization flowchart.
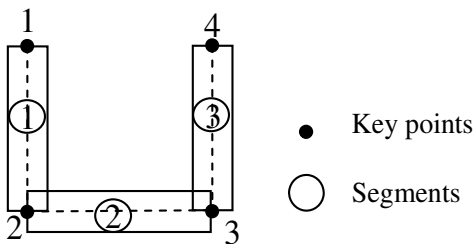
Figure 2. Geometric representation of cold formed steel member

and constraints, which are generally nonlinear functions of the design variables. Design variables, objective function and constraints can be selected based on experience and knowledge about the response. In this study, the objective function is maximization of the critical buckling load subject to constant volume of material constraints. In addition, explicit geometrical constraints are imposed on the design variables to avoid impractical geometries. For example, a minimum element thickness is defined to avoid zero or ' negative' element thickness

values. It is worth mentioning here that the objective function and the constraint hull may be non-convex and therefore local optima may exist.

Shape definition

The definition and control of the geometric model of the cold formed steel members to be optimized is an important task. The cross section of typical cold formed steel member shown in Figure 2 is formed by an assembly of segments. Each segment may be a cubic spline curve passing through certain 'key points' all of which lie on the mid-surface of the structure cross-section. Some key points are common to different segments at their points of intersection. At such intersections one can impose $C(0)$ shape continuity. Alternatively, a smooth continuous curve having $C(2)$ shape continuity can be obtained.

The coordinates may be expressed with reference to the global set of axes or alternatively some locally defined set. Some of the coordinates at the key points may be held constant or frozen. To impose symmetry or to allow for specially constrained shape changes, some of the design variables may be linked through equality constraints.

Selection of shape design variables

The position vectors of the key points used to define the cold formed steel members mid-surface are taken as design variables. The mid-surface of the structure to be optimized is represented by cubic spline curves passing through key points on the structure. The coordinates are given in the global Cartesian coordinates system. The use of the coordinates of key points as design variables leads to fewer design variables and more freedom in controlling the shape of the structure.

Sometimes for practical reasons and computational efficiency, it is necessary to link the design variables at two or more key points to satisfy certain requirements. Linking of design variables also has the following main advantages:

1. The number of design variables is reduced considerably;
2. The movement of a whole segment (as a rigid body) can be treated with a single design variable; and
3. Symmetry of shape can be easily achieved.

Selection of thickness design variables

A similar approach to that adopted for the shape design variables is used in which the thickness values at some
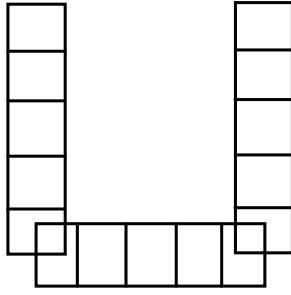
Figure 3. Mesh representations of cold formed steel column.

key points are specified as design variables. In this study due to the production process of cold formed steel structures, constant thickness is used.

Finite strip model

In order to perform such a FS analysis, proper meshing of cold formed steel column cross section is required. Here, we use an automatic mesh generator which allows refinement of FS meshes. It also allows for a significant variation in mesh spacing throughout the region of interest. The mesh generator can generate meshes of two three and four noded elements and strips. Figure 3 shows a mesh example of cold formed steel members.

Structural analysis method

Structures, which are simply supported on diaphragms at two opposite edges with the remaining edges arbitrarily restrained such as cold formed steel members (where the cross section does not change between the simply supported ends) can be analyzed accurately and inexpensively using the FS method in cases where a full finite element analysis could be considered extravagant. In a way, FS method combines the use of Fourier expansions and one-dimensional finite elements to model the longitudinal and transverse structural behavior respectively. Two, three and four noded members of Mindlin Reissner strips were used for buckling analysis of cold formed steel members used. The formulation was shown to be extremely efficient and simple. Note that, FS formulation which is based on the previous work of Özakça et al. (1993), summarized, can be used for buckling analysis of cold formed steel members.

   If we consider the buckling of the Mindlin Reissner shell strip translations in the ℓ, y and n directions can be represented by the displacement components u_ℓ, v_ℓ and w_ℓ. The displacement components u_ℓ and w_ℓ may be written in terms of global displacements u and w in the x and z directions as:

$$u_\ell = u\cos\alpha + w\sin\alpha \quad w_\ell = -u\sin\alpha + w\cos\alpha \quad (1)$$

where α is the angle between the x and l axes.

The strain energy for a typical Mindlin Reissner strip e of length b is given in terms of the global displacements u, v, w and the rotations ϕ and ψ of the mid-surface normal in the ln and yn planes respectively by the expression:

$$U^e = \frac{1}{2}\int_0^b \int_{\ell^e} \left(\varepsilon_m^T \mathbf{D}_m \varepsilon_m + \varepsilon_b^T \mathbf{D}_b \varepsilon_b + \varepsilon_s^T \mathbf{D}_s \varepsilon_s \right) d\ell \, dy \quad (2)$$

where ε_m, ε_b and ε_s are the membrane, bending and transverse shear strains respectively and the matrix of membrane D_m, flexural D_b and shear D_s rigidities are given in Hinton et al. (1993).

Potential energy of the applied in-plane stresses

The potential energy of the applied in-plane stresses σ_ℓ^0, and σ_y^0 is caused by the action of these stresses on the corresponding second order strains and has form:

$$V^e = \frac{1}{2}\int_0^b \int_{\ell^e} \left(t\left\{ \sigma_\ell^0 \left[\left(\frac{\partial u}{\partial \ell}\right)^2 + \left(\frac{\partial v}{\partial \ell}\right)^2 + \left(\frac{\partial w}{\partial \ell}\right)^2 \right] + \sigma_\eta^0 \left[\left(\frac{\partial u}{\partial y}\right)^2 + \left(\frac{\partial v}{\partial y}\right)^2 + \left(\frac{\partial w}{\partial y}\right)^2 \right] \right\} \right.$$
$$\left. + \frac{t^3}{12}\left\{ \sigma_\ell^0 \left[\left(\frac{\partial \phi}{\partial \ell}\right)^2 + \left(\frac{\partial \psi}{\partial \ell}\right)^2 \right] + \sigma_\eta^0 \left[\left(\frac{\partial \phi}{\partial y}\right)^2 + \left(\frac{\partial \psi}{\partial y}\right)^2 \right] \right\} \right) d\ell \, dy$$

$$(3)$$

Stiffness matrix

$\mathbf{K}^e$ of strip elements can be evaluated considering the strain energy of the Mindlin Reissner strip. The strain energy of a strip element can be expressed as:

$$U^e = \frac{1}{2}\sum_{p=p_1}^{p_2} \sum_{q=q_1}^{q_2} \sum_{i=1}^{n} \sum_{j=1}^{n} \mathbf{d}_i^p [\mathbf{K}_{ij}^e]^{pq} \mathbf{d}_j^q \quad (4)$$

where the typical sub-matrix of the stiffness $\mathbf{K}^e$ of strip e linking nodes i and j and harmonics p and q has the form:

$$[\mathbf{K}_{ij}^e]^{pq} = \int_0^b \int_{-1}^{+1} \left([\mathbf{B}_{mj}^p]^T \mathbf{D}_m \mathbf{B}_{mj}^q + [\mathbf{B}_{bj}^p]^T \mathbf{D}_b \mathbf{B}_{bj}^q + [\mathbf{B}_{sj}^p]^T \mathbf{D}_s \mathbf{B}_{sj}^q \right) J \, d\xi \, dy$$

$$(5)$$

In which $\mathbf{B}_{mi}^p$, $\mathbf{B}_{bi}^p$ and $\mathbf{B}_{si}^p$ are the membrane, bending and shear strain–displacement matrices associated with harmonic p, node i as given in Hinton et al. (1993) together with Jacobian term J.

Geometric stiffness matrix

We can now evaluate the geometric stiffness matrix $\mathbf{K}_\sigma^e$ associated with the potential energy V^e of the applied inplane stresses σ_ℓ^0 and σ_y^0 which can be expressed as:

$$V^e = \frac{1}{2} \sum_{p=p_1}^{p_2} \sum_{q=q_1}^{q_2} \sum_{i=1}^{n} \sum_{j=1}^{n} \mathbf{d}_i^p [\mathbf{K}_{\sigma ij}^e]^{pq} \mathbf{d}_j^q \qquad (6)$$

If the structure geometry is well modeled, then such a formulation yields and upper, bound to the magnitude of the true buckling load. The 'true' buckling load is the linear bifurcation load of the structure in its reference configuration; it is not necessarily the collapse load of the actual structure. The FS formulation given in this section yields the 'true' buckling load. The geometric stiffness matrices can be written as:

$$[\mathbf{K}_{\sigma ij}^e]^{pp} = \int_0^b \int_{-1}^{+1} \left(t[\mathbf{S}_{ui}^p]^T \mathbf{H} \mathbf{S}_{uj}^p + t[\mathbf{S}_{vi}^p]^T \mathbf{H} \mathbf{S}_{vj}^p + t[\mathbf{S}_{wi}^p]^T \mathbf{H} \mathbf{S}_{wi}^p \right)$$

$$\left(\frac{t^3}{12} [\overline{\mathbf{Q}}_i^p]^T \mathbf{H} \overline{\mathbf{Q}}_j^p + \frac{t^3}{12} [\overline{\mathbf{R}}_i^p]^T \mathbf{H} \overline{\mathbf{R}}_j^p \right) J d\xi \, dy \qquad (7)$$

in which $\mathbf{S}_{ui}^p$, $\mathbf{S}_{vi}^p$, $\mathbf{S}_{wi}^p$, $\mathbf{Q}_i^p$, $\mathbf{R}_i^p$ and $\mathbf{H}$ matrices associated with harmonic p, node i as given in Hinton et al. (1993).

Note that, $[\mathbf{K}_{ij}^e]^{pq}$ and $[\mathbf{K}_{\sigma ij}^e]^{pq} = 0$ if $p \neq q$ because of the orthogonality conditions. Due to orthogonality relation, on assembly of the contributions to the total potential energy $U + V$ from all of the strips and subsequent minimization with respect to the nodal values, the following eigenvalue expression is obtained for each harmonic p :

$$[\mathbf{K}^{pp} + \lambda^p \mathbf{K}_\sigma^{pp}] \overline{\mathbf{d}}^p = 0 \qquad (8)$$

where λ^p is the load factor by which the inplane stress σ_ℓ^0 and σ_y^0 are multiplied to produce instability and $\overline{\mathbf{d}}^p$ is the associated buckling mode. In the present studies the eigenvalues were evaluated using the subspace iteration algorithm. We seek the lowest value of λ^p which provides (8). The lowest value of λ^p generates critical buckling load of structure.

$$P_{cr} = \lambda^p P_0 \qquad (9)$$

where P_0 is applied load.

Sensitivity analysis

Derivative of critical buckling load

The first partial derivatives of the structural response quantities with respect to the shape (or other) variables provide the essential information required to couple mathematical programming methods and structural analysis procedures. In eigenproblems, methods for calculating eigenvalue and eigenvector sensitivity include the finite difference method, the semi-analytical method, the modal method, Nelson's method etc.

In the present study we use semi-analytical method for derivative of critical buckling load. In the FS displacement approach the governing equations for buckling situation may be written as:

$$[\mathbf{K}^{pp} + \lambda^p \mathbf{K}_\sigma^{pp}] \overline{\mathbf{d}}^p = 0 \qquad (10)$$

where the pth harmonic $\mathbf{K}^{pp}$ is the stiffness matrix, $\mathbf{K}_\sigma^{pp}$ is the load matrix, λ^p is the buckling factor and $\overline{\mathbf{d}}_\mathbf{p}$ is the buckling mode shape which is normalized so that:

$$\overline{\mathbf{d}}_p^T \mathbf{K}_\sigma^{pp} \overline{\mathbf{d}}_p = 1 \qquad (11)$$

when the eigenvalues are distinct, the expression for the buckling derivative with respect to design variable s_i can be derived from (10) and (11) so that:

$$\frac{\partial \lambda^p}{\partial s_i} = \overline{\mathbf{d}}_p^T \left(\frac{\partial K^{pp}}{\partial s_i} - \lambda^p \frac{\partial K_\sigma^{pp}}{\partial s_i} \right) \overline{\mathbf{d}}_p \qquad (12)$$

The derivatives are computed by re-calculating $\mathbf{K}^{pp}$ and $\mathbf{K}_\sigma^{pp}$ for a small perturbation Δs_i of the design variable (coordinates or thickness). The derivatives of the stiffness and mass matrices with respect to the design variable s_i may then be written as:

$$\frac{\partial \mathbf{K}^{pp}}{\partial s_i} \approx \frac{\mathbf{K}^{pp}(s_i + \Delta s_i) - \mathbf{K}^{pp}(s_i)}{\Delta s_i} \qquad (13)$$

$$\frac{\partial \mathbf{K}_\sigma^{pp}}{\partial s_i} \approx \frac{\mathbf{K}_\sigma^{pp}(s_i + \Delta s_i) - \mathbf{K}_\sigma^{pp}(s_i)}{\Delta s_i} \qquad (14)$$

Derivative of volume

In the present study, derivative of constraint function
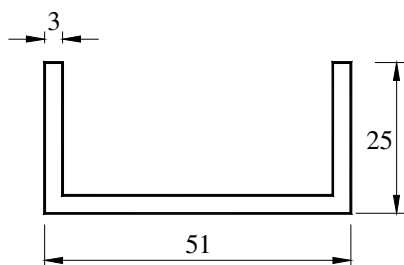
Figure 4. LC plain channel cross section.
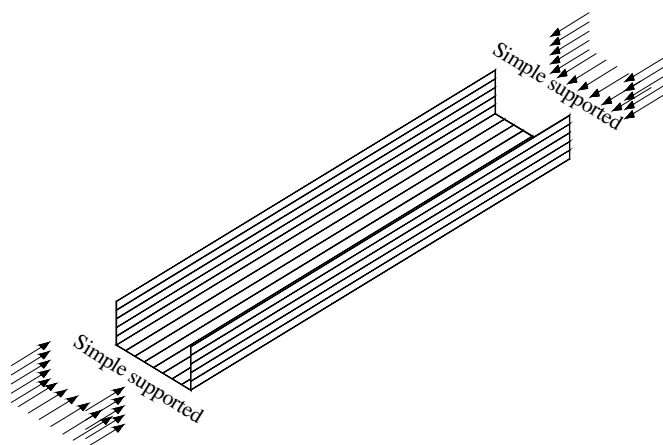
Figure 5. FS model, loading and boundary conditions.

volume is calculated using a forward finite difference approximation:

$$\frac{\partial V}{\partial s_i} \approx \frac{V(s_i + \Delta s_i) - V(s_i)}{\Delta s_i} \qquad (15)$$

where the volume V of the whole structure (or cross-sectional area of the structure may also be used) can be calculated by adding the volumes of numerically integrated FSs.

Mathematical programming

Using the information derived from FS analysis and sensitivity analysis, mathematical programming methods are used to generate new shapes with improved objective functions. Furthermore, the constraints must be satisfied if the new design is to be deemed acceptable. If the convergence criteria for the optimization algorithm are satisfied, then the optimum solution has been found and the solution is terminated.

In structural optimization, various mathematical programming techniques have been extensively applied, with most of the applications based upon one of following algorithms: The method of moving asymptotes, sequential quadratic programming (SQP), penalty function methods or feasible direction methods. In the present work, only the sequential quadratic programming algorithm is used (Svanberg, 1987). No effort has been made to study the mathematical programming methods used in the structural optimization procedures and SQP algorithm is used here essentially as a black box.

Example

We now consider a LC shape profile to demonstrate the ability of the present algorithm to optimize the cold formed steel columns (Figure 4). The column is supported by diaphragms at each end. The objective is to maximize the critical buckling load subject to the constraints that the volume of the panel remains constant and the buckling loads from λ_1 to λ_{10} should be greater than the critical buckling loads. The design improvement procedures are carried out by allowing changes of the thickness and shape parameters so as to maximize the buckling load under the given constant total material volume which is 291000 mm^3.

Figure 4 shows shape and dimensions of the LC shaped cold formed steel column cross section. All dimensions are in milimeter. Optimized column length is considered as 1000 mm. The linear buckling analysis needs material properties such as Elastic modulus and Poisson's ratio. In this study, the elastic modulus of material is $E = 200$ GPa and Poisson's ratio is $v = 0.3$.

Figure 5 illustrates the idealized FS model, loading and boundary conditions of column section. The buckling analyses of column sections performed under axially uniformly distributed pressure loads. Note that uniform compressive load is redistributed according to the changes in element dimensions during optimization process.

The used program has the ability of shape optimization without limitation in number of design variables. As mentioned before, the above three cases were decided to be proper for the generation of applicable cross sections. The structural optimization procedures are applied for three different design variable cases. Types of design variables which are shown in Figure 6 were established by considering applicability and reproducibility of steel columns.

Case I

The cross-sectional shape of the LC plain channel is modeled using 3 segments and 4 key points. Thickness

● fixed key points   ○ movable key points (during optimization)
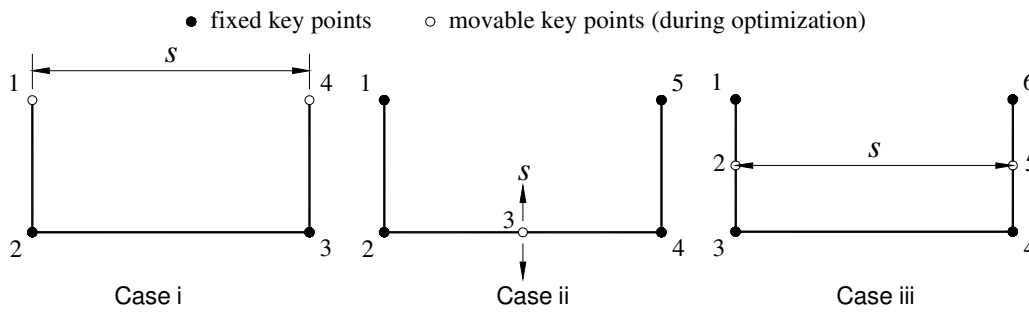
Figure 6. Optimization cases and design variables

Table 1. Optimum design variables and critical buckling loads of cold form steel columns.

Case	Optimum values of design variables		Buckling load	
	s	t	Optimum	% increases
i	17.724	2.732	108.953	21.5
ii	-36.459	2.137	153.016	70.6
iii	89.780	2.013	289.648	223.0

of the profile and *x*-distance between key points 1 and 4 are considered as design variables. That is *x*-coordinate of the key points 1 and 4 are linked so that symmetry is maintained.

Case II

The cross-sectional shape of the LC plain channel is modeled using 4 segments and 5 key points. Thickness of the profile and *y*- coordinate of key point 3 are chosen as design variables (S_2 is midpoint of second segment).

Case III

The cross-sectional shape of the LC plain channel is modeled using 5 segments and 6 key points. Thickness of the profile and *x*-distance between key points 2 and 5 are chosen as design variables. That is, *x*-coordinate of the key points 2 and 5 are linked so that symmetry is maintained. Table 1 presents the optimal values and percentage increases of critical buckling loads. The analyses are carried out using a mesh of 24 cubic strips. The initial critical buckling load of LC column P_{cr} was 89.668 kN. The critical buckling loads are increased by 21.5, 70.6 and 223.0% for each of the three design variables cases (*i*), (*ii*) and (*iii*) respectively.

It is worth mentioning here that, when constraints on the buckling loads are not imposed, the first buckling load λ_1 increases over 300%. However, the critical buckling load occurs at higher modes, n > 1, and reduces to lower values than the initial value. As stated before, this highlights the dangers in optimizing the buckling load. In order to eliminate this problem, modes higher than n > 1 are checked in the present study. The optimized shape and the critical buckling loads are shown in Figure 7 on a graphical illustration.

Post-buckling analysis

Using the finite element method and employing geometric analysis procedures, it is possible to model the local buckling and post buckling failure behavior of cold form steel members. To test the optimized sections on the post-buckling performance of realistic cold form steel section, base profile and three optimized section were selected.

The non-linear finite element analyses were carried out using ANSYS commercial program. The finite element model employed 8-node quadrilateral thick shell elements (MARC type 22). Changes in thickness were modelled as changes in element thickness. For the post-buckling analysis, the mesh was perturbed in the first increment using the first eigenmode, with the amplitude of the chosen deformations 1/1000 of the panel length. Geometric non-linearity was activated but the large strain capability was left deactivated, since little plastic strain was expected. Solution was achieved using the arc length method

In all cases, linear buckling and collapse modes were correctly predicted. The linear buckling loads were under-
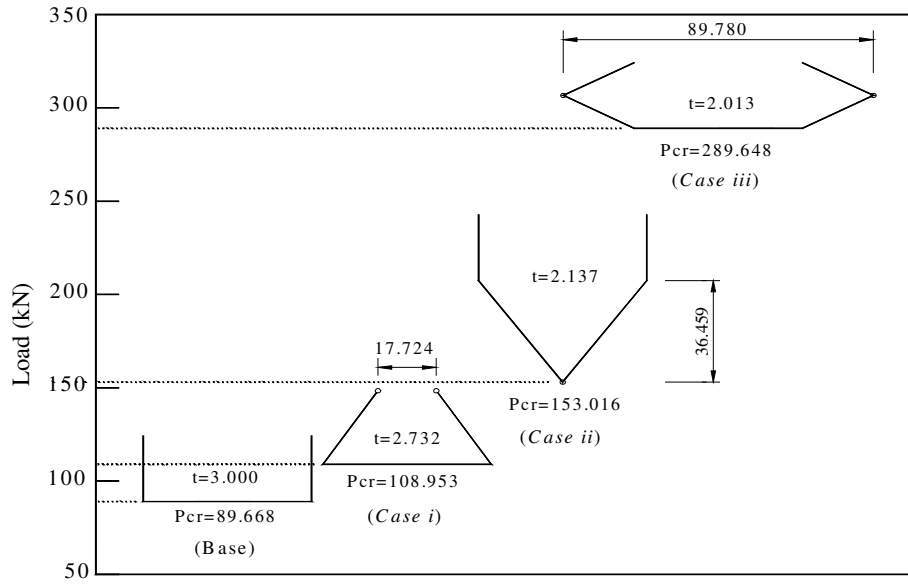
Figure 7. Optimum shapes of cold form steel columns.
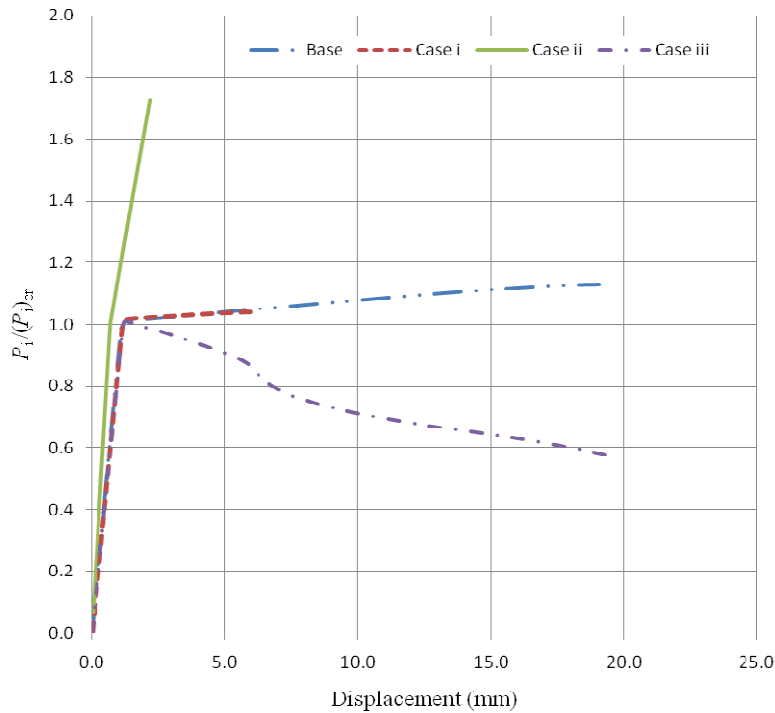
Figure 8. The force end shortening diagram.

underpredicted, (only slightly 6 to 11% depending on the profile). Figure 8 displays the force-end shortening diagram for the base profile and three optimized profile. Figure 8 also shows large gains in collapse load for case ii. The force-end displacement diagrams of case i, arbitrarily conceived base profile. However, the snap through occurred in case iii.

Conclusions

A general structural shape optimization algorithm, based on mathematical programming techniques coupled with a numerical structural analysis method, has been presen-ted. Geometric modeling, automatic mesh generation, FS analysis, behavior sensitivity analysis has been success-

fully applied to the maximization of critical buckling load of cold form steel columns. The following general conclusions may be drawn:

1. The integrated structural optimization algorithm described in this paper is robust and reliable and provides an efficient way of finding optimum shapes for cold form steel columns.

2. The application of structural shape optimization in conjunction with FS analysis is an efficient and effective method, in particular for problems with a great number of design variables and a reasonable number of design constraints.

3. Definition of the shape variables is crucial, that is, the parameterization of the optimization model need to have as few degrees of freedom as possible to simplify the optimization task and as many degrees of freedom as necessary so that the problem is not over-constrained. The optimum solution obtained is only the optimum for this particular problem definition; in only very rare cases will it be the global optimum.

4. Incorrectly formulated optimization problems may lead to designs which at best show very little reserve because of tight constraints margins and at worst are imperfection sensitive and fail prematurely. Also local optima may be produced which are long way from the global optimum. Consequently, care should be taken in the selection of appropriate design variables, the accurate representation of the boundary curves and the selection of the objective function and constraints.

5. All the optimized profile section should be checked against post-buckling. The optimized profile sections can show different post-buckling behavior. The post-buckling stiffness can be increased in some example but in all. The most crucial point is that, the snap through behavior can occur in some optimized profile section.

REFERENCES

Cristopher DM, Schafer BW (2009). Elastic buckling of cold-formed steel columns and beam with holes, Eng. Struct., 31: 2812-2824.

Davies JM, Leach P (1994). First-order generalized beam theory. J. Constructional. Steel. Res., 31: 187-220.

Gardner L, Nethercot DA (2004) Experiments on stainless steel hollow sections—Part 2: Member behaviour of columns and beams. J. Constructional. Steel. Res., 60: 1319-1332.

Hancock GJ (1985). Distortional buckling of steel storage rack columns. J. Struct. Eng. (ASCE). 111: 2770-2783.

Hinton E, Petrinic N, Özakça M (1993). Buckling analysis and shape optimization of variable thickness prismatic folded plates. Part 1: Finite Strip Formulation, Eng. Computations., 10: pp. 483-489.

Karim A, Adeli H (1999). Global optimum design of cold-formed steel hat-shape beams. Thin-Walled. Struct., 35: 275-288.

Kesti J, Davies MJ (1999). Local and distortional buckling of thin-walled short columns. Thin Walled. Struct., 34: 115-134.

Kwon YB, Hancock GJ (1992). Tests of cold-formed channels with local and distortional buckling, J. Struct. Eng. (ASCE). 118: 1786-1803.

Kwon YB, Hancock GJ. (1991). A nonlinear elastic spline finite strip analysis for thin-walled sections. Thin Walled. Struct., 12: pp. 295-319.

Lau SCW, Hancock GJ (1987). Distortional buckling formulas for channel columns. J. Struct. Eng. (ASCE). 113: 1063-1078.

Lee J, Kim SM, Park HS (2006). Optimum design of cold formed steel columns by using micro genetic algorithms. Thin-Walled. Struct., 44: 952-960.

Lu W (2002). Optimum design of cold-formed steel purlins using genetic algorithms. PhD Thesis, Helsinki University of Technology.

Pignataro M, Pasca M, Franchin P (2000). Post-buckling analysis of corrugated panels in the presence of multiple interacting modes. Thin-Walled. Struct., 36(1); 47-66.

Pu Y, Godley MHR, Beale RG, Lau HH.(1999) Prediction of ultimate capacity of perforated lipped channels, J. Struct. Eng. (ASCE). 125(5): 510-514.

Schafer BW, Peköz T (1998). Computational modeling of cold formed steel: characterizing geometric imperfections and residual stresses. J. Constructional. Steel. Res., 47: 193-210.

Seaburg PA, Salmon CG (1971). Minimum weight design of light gage steel members. J. Struct. Division. (ASCE). 97(1): 203-222.

Talja A, Salmi P (1995). Design of stainless steel RHS beams, columns and beam–columns. VTT Research Notes 1619. Espoo: Technical Research Centre of Finland.

Young B, Hartono W (2002). Compression tests of stainless steel tubular members. J. Struct. Eng., (ASCE). 128(6): 754-761.